Transfer function for the seismic signal recorded in solid and fractured rock surrounding deep level mining excavations

by A. Cichowicz*, A.M. Milev†, and R.J. Durrheim†

Synopsis

The objective of this work is to quantify the effect of the rock mass surrounding a stope or a tunnel on the seismic signal so that the rockburst damage on the excavation can be derived. It has been shown that the transfer function of rock mass surrounding an excavation can be modelled using a damped oscillator. The method of estimating the transfer function is extended in this paper. The parameters of a damped oscillator are estimated using inversion techniques and the transfer function is modelled as a time-varying system. The technique is tested on data acquired at three different sites in two deep gold mines. Employment of a modal model of the transfer function was suitable in two cases. Application of this technique is essential to track the time variation of the natural frequency during ground motion caused by a seismic event.

Identification of dynamic structural systems

The objective of this study is to quantify the effect of the rock mass surrounding a stope or tunnel on the seismic signal. The characterization of the seismic ground motion is needed to engineer rockburst resistant excavations. Work done as part of this study shows that the transfer function of the rock mass surrounding an excavation can be modelled using a model comprised of damped oscillator (Cichowicz *et al.*[1]). The system identification method is used to estimate the parameters of the damped oscillators.

Ljung and Soderstrom[2] and Ljung[3] studied methods for the time-domain identification of linear multi-degree of freedom of structural dynamic systems. The term identification refers to the determination of analytical models for structure, based on the observations of the system. Recordings of a single input and single output are sufficient to determine all the modal frequencies and damping coefficients in a structure (Safak[4]).

The equivalent discrete-time equation for a single input, single output dynamic system can be written in the following form:

$$\begin{aligned} &y(t) + a_1 y(t-1) \\ &+ \ldots + a_i y(t-l) = b_1 u(t-1) \\ &+ \ldots + b_m u(t-m) \end{aligned} \qquad [1]$$

where: $u(t)$ and $y(t)$ are the input and output sequences, respectively; a_i and b_i are constants for time-invariant systems, and functions of time for time-varying systems. Although the equation represents a linear system, it has been suggested that any non-linear system can also be represented by a similar equation with time-varying parameters (a_i, b_i).

The system transfer, $H(q)$, is defined as the polynomial ratio $B(q)/A(q)$ were,

$$A(q) = 1 + a_1 q^{-1} + \ldots + a_i q^{-1} \qquad [2]$$

$$B(q) = b_1 q^{-1} + \ldots + b_m q^{-m} \qquad [3]$$

and

q^{-i} is a backward-shift system operator defined as $q^{-i} y(t) = y(t-i)$,

Equation [1] can be written in a more compact form as:

$$y(t) = \frac{B(q)}{A(q)} u(t) \qquad [4]$$

The polynomial ratio $B(q)/A(q)$ is called the system transfer operator, $H(q)$. Discrete-time equations can also be expressed in the frequency domain by taking the Z-transform. The Z-transform of both sides in Equation [4] can be written as:

$$Z[y(t)] = \frac{B(z)}{A(z)} Z[u(t)] \qquad [5]$$

* *Department of Geophysics, University of the Witwatersrand, Private Bag 3, Wits 2050, Johannesburg.*

† *CSIR: Division of Mining Technology, P.O. Box 91230, Auckland Park, 2006.*

 SA ISSN 0038–223X/3.00 + 0.00. Paper received Apr. 1998; revised paper received Jul. 1999.

where $Z[y(t)]$ = the Z-transform and z is any complex number. The polynomials $A(z)$ and $B(z)$ are the same as defined by Equations [2] and [3] except all the q's are replaced by z's. The transfer function can be represented in terms of harmonic functions by selecting, $z = \exp(i2\pi f\Delta t)$, where f denotes the frequency and Δt is the sampling interval.

The stability conditions require that the roots of the denominator polynomial $A(z)$ should all have a magnitude less than one. This means that the roots of $A(z)$ are all in complex-conjugate pairs located inside the unit circle in the complex plane. The transfer function can be written as:

$$H(z) = \sum_{j=1}^{l,m/2} H_j(z) \qquad [6]$$

where: l, m are the lengths of the series $u(t)$ and $y(t)$, and

$$H_j(z) = \frac{2R(q_j) \pm 2R(q_j p_j)z^{\pm 1}}{1 \pm 2R(p_j)z^{\pm 1} + |p_j|^2 z^{\pm 2}} \qquad [7]$$

where: $H_j(z)$ is the second order filter, $R(q)$ is the real part of q, p is the complex conjugate, p_j is the complex root of the polynomial $A(z)$ and q_j is the corresponding residual of $H(z)$. The filter output $y(t)$ is modelled as the linear combination of the outputs of second-order filter each subjected to input $u(t)$. The form given by Equation [6] is known as the parallel form of realization. Each second-order filter $H_j(z)$ corresponds to a simple, damped oscillator. The damping d_j and the frequency f_j of each oscillator are defined by the following Equations (Safak[4]):

$$d_j \frac{\ln\left(\frac{1}{r_j}\right)}{\left[F_j^2 + \ln^2\left(\frac{1}{r_j}\right)\right]^{1/2}} \qquad [8]$$

$$f_j = \frac{\ln\left(\frac{1}{r_j}\right)}{2\pi d_j \Delta t} \qquad [9]$$

where: $r_j = |p_j|$, F_j is the modulus and the arguments of the j^{th} pole (or of its complex-conjugate).

The recordings from dynamic systems are always contaminated by noise existing in the recording environment, as well as by the imperfections in the recording instrument. Hence, the following equations for the signal.

$$A(q)y(t) = B(q)u(t) + C(q)e(t) \qquad [10]$$

where:

$$C(q) = 1 + c_1 q^{-1} + \ldots + c_n q^{-n} \qquad [11]$$

and $e(t)$ is a white noise sequence. Equation [10] represents a family of model structures for noise systems. The $A(q)$ corresponds to poles that are common between the dynamic model and the noise model. The motivation for introducing $C(q)$ polynomial is to provide more flexibility in the noise descriptions.

Recursive prediction error methods

System identification constitutes determining the coefficients of the polynomials in $A(z)$, $B(z)$ and $C(z)$ for a given pair of input and output sequences:

$$\Omega = (a_1,\ldots,a_l,b_1,\ldots,b_m,c_1,\ldots,c_n) \qquad [12]$$

The one step ahead prediction $y_{pred}[t, u(t), a_i, b_i, c_i]$ of $y(t)$ at time t is based on the past values of input $u(t)$, output $y(t)$, and parameters a_i b_i c_i. The difference,

$$E(t,\Omega) = y(t) - y_{pred}(t,\Omega) \qquad [13]$$

gives the error in the estimation at time t. System identification aims to determine the vector, Ω, such that the total error $\Sigma E^2(t,\Omega)$ is minimum. The most convenient way of measuring the total estimation error is the least squares method. The least squares method uses quadratic criteria for measuring errors. A weighting factor (forgetting factor) is also included in the criteria.

$$E = \sum_k^1 L^{1-k} E^2(t,\Omega) \qquad [14]$$

where: L is the forgetting factor.

Measurements that are older carry less weight in [14] than the current values. For time-invariant systems, weighting factors can all be taken as equal to one. For time-varying systems, weighting factors are essential to track the time variation of system parameters. The forgetting factors localize the identification by giving more weight to the current values, and by gradually discounting the past values. A recursive identification algorithm is:

$$\Omega(t) = \Omega(t-1) + K(t)[y(t) - y_{pred}(t)] \qquad [15]$$

where: $\Omega(t)$ is the parameter estimate at time t, and $y(t)$ is the observed output at time t; $y_{pred}(t)$ is a prediction of the value $y(t)$ based on observation up to time $t-1$. The gain $K(t)$ determines in what way the current prediction error $y(t) - y_{pred}(t)$ affects the update of the parameter estimation. In this work the *Matlab*[5] implementation of Equation [15] is used.

Analysis of the field data

Experiment 1 (footwall drive: Blyvooruitzicht Gold Mine)

Data from the experiment with two geophones were used to study the transfer function of the rock mass surrounding an excavation. The geophones were installed in close proximity to each other; the first in solid rock and the second in a footwall drive. Figure 1 shows an example of ground motion recorded in solid rock (solid line) and recorded in a footwall drive (dotted line). The velocity spectrum of the geophone in solid rock is exactly as the theory predicts (Brune[6]), (see Figure 2—solid line). The geophone installed in the footwall drive shows very clear resonance frequencies (see Figure 2—dotted lines).

The transfer function of the site effect is calculated using the method described in the previous section of this work. To improve modelling precision it is good practice to remove very high frequency contents from a signal using the low pass Butterworth filter. To preserve the shape of the signal a zero-phase filter is applied by processing in both the forward and reverse directions. Parameters of transfer function were calculated for several orders of $A(q)$, $B(q)$ and $C(q)$ polynomials.

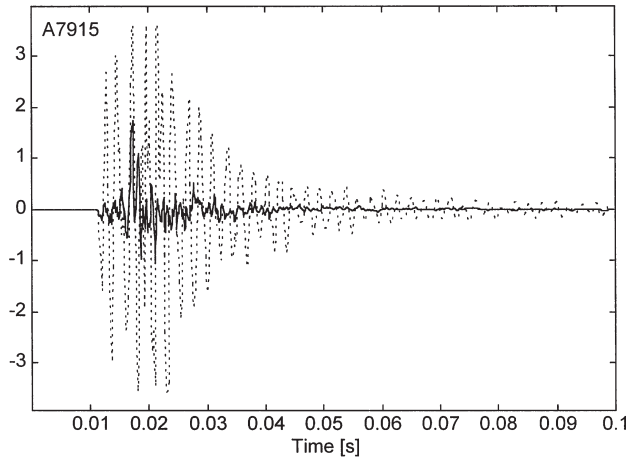

Figure 1—An example of real seismograms (Experiment 1—footwall drive: Blyvooruitzicht Gold Mine; event A7915), recorded in solid rock—solid line, and recorded in a footwall drive—dotted line

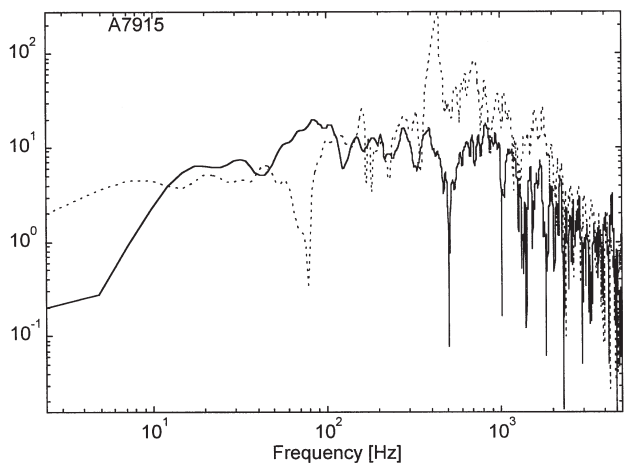

Figure 2—Velocity spectrum of the seismograms (Experiment 1—footwall drive: Blyvooruitzicht Gold Mine; event A7915) recorded in a solid rock—solid line, and recorded in a footwall drive—a dotted line

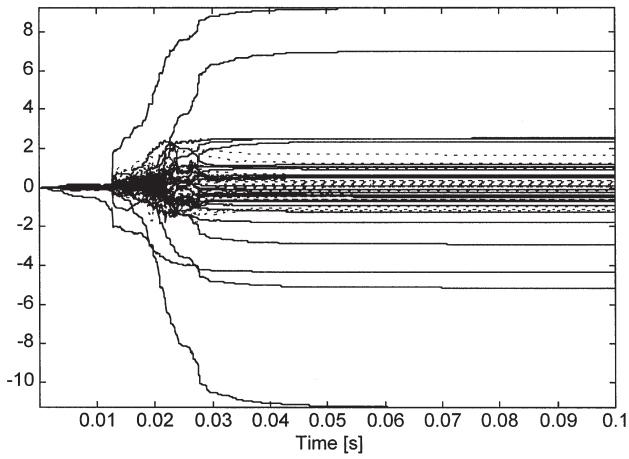

Figure 3—The coefficients of the polynomials *A (q)* and *B (q)* as a function of time

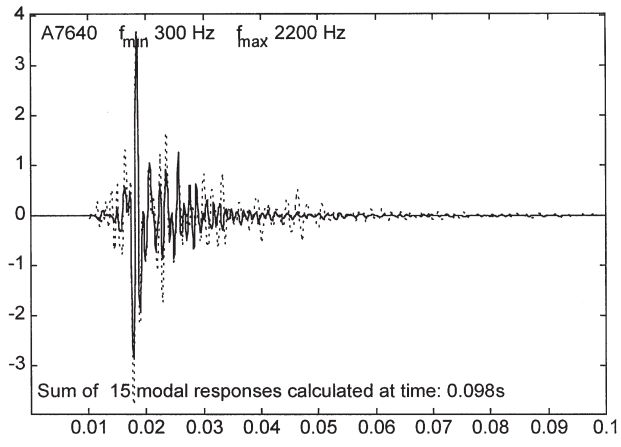

Figure 4—Sum of 15 modal responses using coefficients calculated at time 0.098 s; a solid line marks the real ground motion and a dotted line marks the calculated ground motion

The transfer function is defined by coefficients of $A(q)$ and $B(q)$ polynomials. Figure 3 shows the coefficient of polynomial $A(q)$ and $B(q)$ versus time. The forgetting parameter is equal to 1.0. The initial part of the time series (from 0 s to 0.01 s) should be ignored, as the learning time for the filter. The next part (from 0.01 s to 0.03 s) shows some significant changes in all coefficient values. This suggests that the P-wave caused the non-linear response of the system. During the vibration caused by the P-wave there is no interval of time with fixed values of coefficient. The arrival of the P-wave shows initial abrupt changes (0.015 s) and then the coefficient stabilizes at time 0.035 s. It is difficult, however, to separate the effect of the adapting coefficient due to the adaptive algorithm from a non-linear response of the system.

The mode contribution to ground motion can be obtained by combining Equations [4] and [6]. The sum of the contribution from each of the modes to the response is plotted in Figure 4 along with the recorded response. However, some modes are fairly close and have different phases. Therefore, when they are added together, most of the amplitudes cancel each other and do not appear in the final response. Figure 4 shows the sum of 15 modal responses using the coefficients calculated at the time of 0.0980 s; the match with the real ground motion is very good. As expected (see Figure 3) a transfer function calculated at the end of seismogram is not suitable for modelling of the P-wave pulse.

Figure 5 shows the real and calculated spectra of the seismograms shown in Figure 4. The spectral match of both signals is obvious. The match can be used as an independent verification of the inversion method. The third curve is the transfer function in frequency domain.

The same calculation of transfer function was repeated for 5 pairs of seismograms. Table I shows modal frequencies and damping coefficients obtained at the end of seismogram for all five pairs of events. The first row of Table I shows a number of seismic events and a frequency range for which calculation was performed. It is encouraging that the main features of the transfer function are similar in all examples.

An examination of Table I shows that the modal frequencies of 400 Hz +/- 20 Hz and 740 Hz +/- 20 Hz are present in all models of the transfer function. The modal

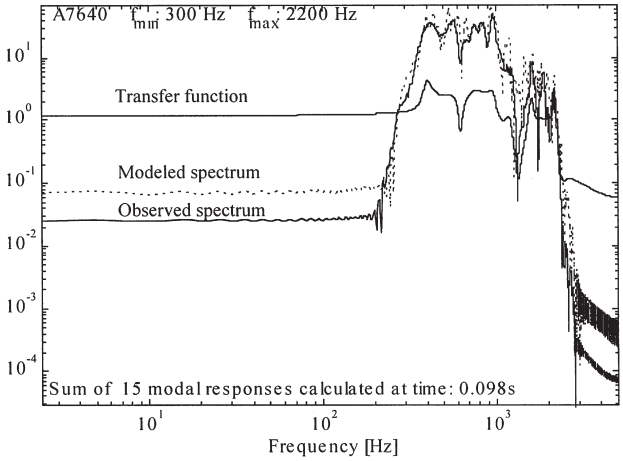

Figure 5—The spectrum of the seismograms from Figure 4 and their transfer function

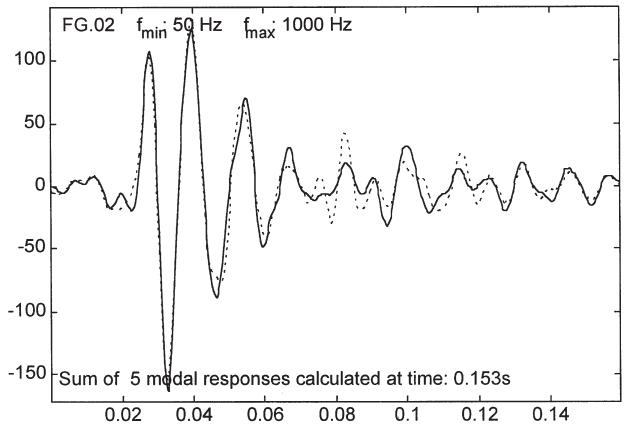

Figure 6—Sum of five modal responses calculated at time 0.153 s (Experiment 2—stope: Vaal Reefs No. 5 shaft; event FG.02); a solid line marks the real ground motion and a dotted line marks the calculated ground motion

Table I

Modal frequencies and damping coefficients for five pairs of seismograms, recorded in solid rock and on the sidewall of a footwall drive

Modal frequencies (Hz) and damping coefficient				
No. A7915 300–2200 Hz	No. A7640 300–2200 Hz	No. A8114 300–2200 Hz	No. A8328 300–2200 Hz	No. A9112 300–2200 Hz
426 Hz 0.032	399 Hz 0.048	425 Hz 0.014	380 Hz 0.056	413 Hz 0.051
			456Hz 0.312	425 Hz 0.611
532 Hz 0.082	611 Hz 0.077			
746 Hz 0.064	764 Hz 0.200	741 Hz 0.189	731 Hz 0.074	718 Hz 0.035
1038 Hz 0.029	971 Hz 0.047	837 Hz 0.125	1006 Hz 0.044	985 Hz 0.021
1350 Hz 0.163		1303 Hz 0.319		1371 Hz 0.091
1532 Hz 0.044				
1803 Hz 0.039			1711 Hz 0.022	1683 Hz 0.025

frequency located between 837 Hz and 1038 Hz is also present in all models of the transfer function.

There are also several other modes with significant amplitudes. Those modal frequencies may vary from model to model of the transfer function. This can be caused by either, the imperfection in the inversion process, or by the different response of site.

Experiment 2 (Vaal Reefs No. 5 Shaft)

Two geophones were installed in the hangingwall of a stope; one close to a support unit and another 1.1 m away.

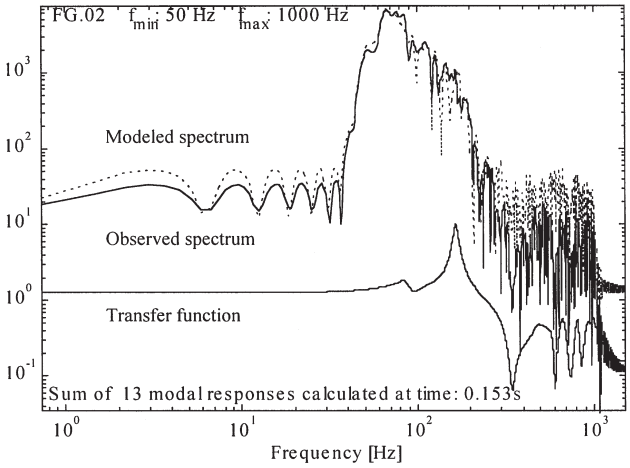

Figure 7—The spectrum of the seismograms from Figure 6 and their transfer function

Table II

Modal frequencies and damping coefficients for data recorded at two points of the hangingwall, May 1997

Modal frequencies (Hz) and damping coefficients: May 1997							
FG02 50-1000Hz	FG03 30-1000Hz	FG04 50-1000Hz	FG05 50-1000Hz	FG06 50-1000Hz	FG07 50-1000Hz	FG08 50-1000Hz	FG09 50-1000Hz
	59 0.072						
103 0.229		142 0.791				130 0.183	
176 0.115		172 0.013	152 0.066	155 0.055	163 0.098		153 0.126
			289 0.242				
			358 0.140	317 0.304	321 0.076		355 0.154
583 0.056	477 0.399		592 0.082	536 0.324	519 0.097	480 0.150	507 0.120
794 0.034	722 0.114	964 0.512			858 0.111	844 0.192	875 0.044

Table III

Modal frequencies and damping coefficients for data recorded at two points of the hangingwall, June 1997

Modal frequencies (Hz) and damping coefficients: June 1997						
FG100 30-500Hz	FG101 30-500Hz	FG102 30-500Hz	FG126 30-500Hz	FG127 30-500Hz	FG128 30-500Hz	FG129 90-500Hz
160 0.392			138 0.089	136 0.081	147 0.087	145 0.070
185 0.103	181 0.116	172 0.040				
	257 0.482	281 0.072	241 0.148	223 0.082	297 0.161	253 0.011
			365 0.101	393 0.127		
				468 0.072	431 0.050	404 0.051

The inspection of seismograms and their spectra shows strong similarity between the two seismograms and spectra. Only after processing of the data it was possible to quantify the difference between them.

The transfer function was well modelled in several cases, as the modal response matches the real response of the system (see Figure 6). In several cases there was a problem with the modelling of initial pulse using the transfer function obtained at the end of ground motion, as discussed above, the non-linear effect may be an explanation.

Some examples are more difficult. The inversion process can only reproduce the main feature of real waveform.

The transfer functions in all examples are very similar. The dominant frequency is around 150 Hz +/- 20 Hz, (see Figure 7) and the second peak in transfer functions is between 200 Hz – 300 Hz (see Table II and Table III).

Table II shows data recorded in May 1997 and Table III shows data collected in June 1997. There is an evident decrease of the first and second modal frequencies in Table III compared to Table II. This observation is extremely important and can be used as a tool to monitor the changes in site conditions. The number of seismic events processed in Table II and Table III is too small to make a convincing statement, however, it can be used as an indication of a trend. In future research, the same type of seismic source should be used to study the changes in site effect.

Experiment 3 (stope: Vaal Reefs No. 5 Shaft)

Two geophones were used in Experiment 3: the first geophone was installed on the hangingwall and the second on the footwall (The hangingwall geophone is the same as the geophone from Experiment 2.) Table IV shows modal frequencies for five pairs of seismograms.

The common feature is the presence of modal frequency around 150 Hz. However, the calculated and the real motion do not match very well (Figure 8). It is only in a few cases that the calculated response overlaps with real ground motion. The dominant peak in transfer function relates to the lowest modal frequency (see Table IV). Figure 9 shows the

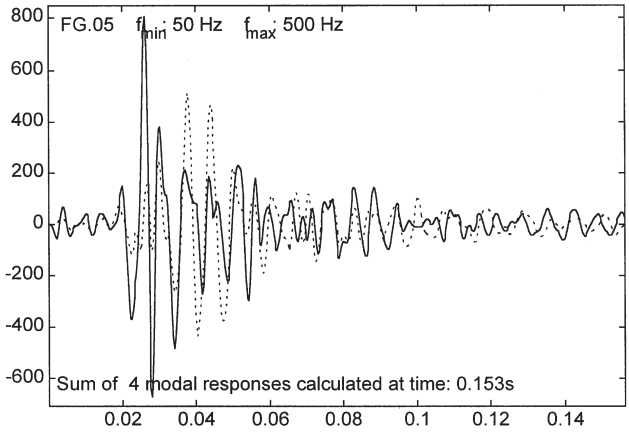

Figure 8—Sum of four modal responses calculated at time 0.153 s, (Experiment 3—stope: Vaal Reefs No. 5 shaft; event FG.05); a solid line marks the real ground motion and a dotted line marks the calculated ground motion

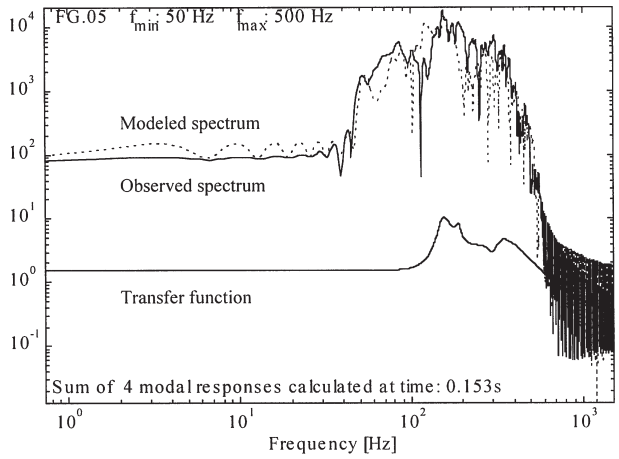

Figure 9—The spectrum of the seismograms from Figure 8 and their transfer function

Table IV

Modal frequencies for five pairs of seismograms recorded on the hangingwall and on the footwall

Modal Frequencies (Hz)				
FG02	FG03	FG04	FG05	FG100
	48			
80				
		111		
155	153	132	154	154
		165	189	264
			305	
			363	381

real and calculated spectra of the seismograms shown in Figure 8. The spectral match is better than the match of the seismograms. The position of this peak changes significantly from model to model of the transfer function. At this stage of understanding, the transfer function in Experiment 3 cannot be modelled using series of damped oscillators.

Conclusions

Time-varying transformations have been used to model the seismic ground motion of the rock surrounding the excavations in deep level gold mines. This approach enables the site response to be characterized in respect of modal frequencies and damping coefficients.

Experiment 1 (footwall drive: Blyvooruitzicht Gold Mine)

- The models of the transfer function are reliable, as the models are similar for all analysed seismic events.
- The first pulse of the seismogram has a different transfer function from the rest of record. This could be an indication that the initial behaviour of the site is non-linear.

Experiment 2 (stope: Vaal Reefs No. 5 Shaft)

- The influence of support on vibration in the hangingwall is measurable. The algorithm presented in this work estimated different vibrations in the different sites in the hangingwall. The obtained model of transfer function is reasonable.
- There is a strong indication that the model frequencies and the damping coefficient of the sites are changing with time (weeks).

Experiment 3 (stope: Vaal Reefs No.5 Shaft)

- The difference between the motion of the footwall and motion of the hangingwall cannot be properly modelled with modal transfer function.

Acknowledgements

This work was part of the research programme supported by SIMRAC under the project GAP 201. We would like to thank the management Blyvooruitzicht Gold Mine and Vaal Reefs No. 5 Shaft for permission to carry out these experiments. The authors thank Dr S. M. Spottiswoode for his helpful review and discussions.

References

1. Cichowicz, A. and Durrheim, R.J. The Site Response of the Tunnel Sidewall in a Deep Gold Mine, Analysis in the Time Domain, In: R.G. Gürtunca and T.O. Hagan (Eds.), *Proc. 1st Southern African Rock Eng. Symp.* Johannesburg, South Africa. 1997. pp. 56–61.
2. Ljung, L. and Soderstrom, T., Theory and practice of recursive identification. *MIT Press*, Cambridge, MA, U.S.A. 1983.
3. Ljung, L., System Identification. Prentice-Hall Inc., Englewood Cliffs, N.J. U.S.A. 1987.
4. Safak, E. Adaptive modelling, Identification, and Control of Dynamic Structure Systems, *Journal of Engineering Mechanics,* vol. 115, 1989 pp. 2386–2405.
5. System Identification Toolbox, Editor Ljung L. *The MathWorks, Inc.* 1997.
6. Brune, J.N., Tectonic stress and the spectra of seismic shear waves from earthquakes, *J. Geophys. Res.*, 75, 1970. pp. 4997–5009. ◆

SABS takes over CSIR's coal preparation programme

The SABS has recently taken over the CSIR's Coal Preparation Programme (CPP), which, from now on, will be known as the SABS's Coal Exploration and Technology Department. The department will become part of the SABS's Coal and Mineral Services Division, although it will remain on the CSIR's Scientiae site and will continue to serve its existing customers.

'Combined with the SABS's Coal Laboratories at Richards Bay and Twistdraai (at Secunda), this will now offer customers a comprehensive pit-to-port coal testing service', said Eugene Julies, President of the SABS. 'This merger of interests is an example of how synergies can result from better cooperation between South African organizations, particularly science councils like the SABS and the CSIR.'

'We must never forget that our organizations exist for one reason and one reason only: to serve our customers' said Dr Geof Garrett, President of the CSIR. 'As South Africa is increasingly opened up to international competition, we will need a team-based approach to formulate structures that can best serve South African industry', he concluded.

'The coal industry welcomes this development', said John Bekker, Senior Manager of SABS Coal and Mineral Services. 'For the first time, the coal industry can now deal with one organization from the very early stages of the exploration and feasibility studies needed for the determination of coal quality, right through to the final certification of a load of coal heading for a particular export destination.'

Additional information can be obtained from Ricky Pinheiro, Manager of the SABS Coal Exploration and Technology Department (at tel (012) 841-4961) and from Johan Bekker, Senior Manager of SABS Coal and Mineral Services Division (at tel (0351) 977-213).